

# Approximate theory of temperature coefficient of resistivity of amorphous semiconductors

Ming-Liang Zhang and D. A. Drabold

*Department of Physics and Astronomy, Ohio University, Athens, Ohio 45701, USA*

(Received 20 December 2011; published 29 March 2012)

In this paper, we develop an approximate theory of the temperature coefficient of resistivity (TCR) and conductivity based upon the recently proposed microscopic response method. By introducing suitable approximations for the lattice dynamics, localized and extended electronic states, we produce explicit forms for the conductivity and TCR, which depend on easily accessible material parameters. The theory is in reasonable agreement with experiments on *a*-Si:H and *a*-Ge:H. A long-standing puzzle, a “kink” in the experimental  $\log_{10} \sigma$  versus  $1/T$  curve, is predicted by the theory and attributed to localized to extended transitions, which have not been properly handled in earlier theories.

DOI: [10.1103/PhysRevB.85.125135](https://doi.org/10.1103/PhysRevB.85.125135)

PACS number(s): 71.23.An, 71.38.Fp, 71.38.Ht

## I. INTRODUCTION

The temperature coefficient of resistivity (TCR) of an amorphous semiconductor (AS) is not only an important quantity in transport theory, but also a critical parameter controlling the sensitivity of uncooled microbolometers employed in thermal imaging “night-vision” applications.<sup>1,2</sup>

The conventional approach to transport coefficients is the kinetic method (Boltzmann or master equations, etc.). However, this is not applicable even to crystalline semimetals and semiconductors (the so-called Landau-Peierls criterion).<sup>3-5</sup> Comparing to metals, the low carrier concentration in these materials results in a lower kinetic energy of carriers. Thus, neither the elastic scattering by disorder nor the inelastic scattering by a phonon has a well-defined transition probability per unit time.<sup>3-5</sup> In AS, the strong electron-phonon interaction of localized states requires a reorganization of the vibrational configuration for any transition involving localized state(s).<sup>6,7</sup> For these intrinsic multiphonon transitions, the energy conservation between initial and final electronic states (a basic condition of Fermi’s golden rule)<sup>3-5</sup> is violated more seriously than that for single-phonon emission and absorption.

In addition, transitions between localized and extended states (LE and EL) are not treated adequately in a kinetic approach. The Miller-Abrahams theory<sup>8</sup> and its extensions suppose that LE and EL transitions do not directly contribute to conduction, and only maintain the distribution of carriers between localized states and extended states in thermal equilibrium (when an external electric field is absent) or in the nonequilibrium stationary state (when an external field is present). Electrical conduction is fulfilled by the transition from a localized state to another localized state (LL) and the transition from an extended state to another extended state (EE).<sup>1,2,9</sup> The theory of phonon-induced delocalization and the theory of transient current excited by photon have heuristically estimated conductivity from LE and EL transitions.

Rigorous expressions for the conductivity and Hall mobility in AS have been obtained in the microscopic response method (MRM).<sup>7,10</sup> These expressions require transition amplitudes rather than transition probability per unit time.<sup>11</sup> Thus, the long-time limit required in a kinetic approach<sup>3,4</sup> is avoided. To the lowest-order self-consistent approximation, there are 29 processes contributing to conductivity and 10 processes contributing to Hall mobility.<sup>7</sup> For example, in an *n*-doped

AS, the conductivity from LE transitions driven solely by an external field is<sup>7</sup>

$$\begin{aligned} \left\{ \begin{array}{l} \text{Re} \\ \text{Im} \end{array} \right. \sigma_{\alpha\beta}(\omega) = -\frac{N_e e^2}{2\Omega_s} \sum_{AB} \text{Im} \frac{(w_{AB}^\alpha - v_{BA}^\alpha)(v_{BA}^\beta)^*}{(E_A^0 - E_B^0)} \\ \times i[I_{BA+} \pm I_{BA-}] [1 - f(E_B^0)] f(E_A^0), \quad (1) \\ \alpha, \beta = x, y, z \end{aligned}$$

where the real part takes the upper sign, and the imaginary part the lower sign.  $\Omega_s$  is the physical infinitesimal volume element used to take spatial average. An AS can be viewed as uniform when we measure its properties (e.g., conductivity) at a linear length scale larger than<sup>12</sup> 10 nm. If we take  $\Omega_s$  as a sphere with a radius larger than 5 nm, then the choice of the center *s* of  $\Omega_s$  inside the AS will not affect<sup>7,10</sup>  $\sigma_{\alpha\beta}$ .  $N_e$  is the number of carriers in the conduction band inside  $\Omega_s$ , and  $f$  is the Fermi distribution function. The velocity matrix elements in Eq. (1) are defined by

$$v_{BA}^\alpha = -\frac{i\hbar}{m} \int d^3x \chi_B^*(\mathbf{r}) \frac{\partial}{\partial x_\alpha} \phi_A(\mathbf{r} - \mathbf{R}_A) \quad (2)$$

and

$$w_{AB}^\alpha = -\frac{i\hbar}{m} \int d^3x \phi_A(\mathbf{r} - \mathbf{R}_A) \frac{\partial}{\partial x_\alpha} \chi_B^*(\mathbf{r}), \quad (3)$$

where  $E_A^0$  and  $\phi_A$  are the eigenvalue and eigenfunction of localized state *A*. We will use letter *A* with or without a natural number subscript to denote a localized state; similarly  $E_B^0$  and  $\chi_B$  are the eigenvalue and eigenfunction of extended state *B*.  $I_{B_1 A_\pm}$  arise from integrating out the vibrational degrees of freedom, and are functions of external field frequency  $\omega$ :

$$\begin{aligned} I_{B_1 A_\pm}(\omega) = \exp \left\{ -\frac{1}{2} \sum_{\alpha} \coth \frac{\beta \hbar \omega_{\alpha}}{2} (\theta_{\alpha}^A)^2 \right\} \\ \times \int_{-\infty}^0 ds e^{is(\pm\omega + \omega_{AB_1})} \exp \left\{ \frac{1}{2} \sum_{\alpha} (\theta_{\alpha}^A)^2 \right. \\ \left. \times \left[ \coth \frac{\beta \hbar \omega_{\alpha}}{2} \cos s\omega_{\alpha} - i \sin s\omega_{\alpha} \right] \right\}, \quad (4) \end{aligned}$$

where  $\omega_{AB} = (E_A^0 - E_B^0)/\hbar$ ,  $\omega_{\alpha}$  is the frequency of the  $\alpha$ th ( $\alpha = 1, 2, \dots, 3\mathcal{N}$ ) normal mode, and  $\mathcal{N}$  is number of atoms inside  $\Omega_s$ . Denote  $\Theta_{\alpha}^A$  as the shift in the origin of the

$\alpha$ th mode induced by the electron-phonon (e-ph) interaction in a localized state<sup>6,7</sup>  $A$ ,  $\theta_\alpha^A = \Theta_\alpha^A (M_\alpha \omega_\alpha / \hbar)^{1/2}$ . To make the narration specific, we hereafter discuss conduction-band transport only. For transport processes in the valence band, one may repeat the discussion *mutatis mutandis*.

To calculate conductivity strictly, one needs (i) the eigenvalues and eigenvectors of single-electron states and (ii) the eigenfrequencies and eigenvectors of the normal modes and the electron-phonon coupling. These can be approximately obtained by one step of *ab initio* molecular dynamics for an optimized configuration. Then, one can compute (i)  $v_{BA}^\alpha$  for all localized states and extended states; (ii)  $\theta_\alpha^A$  for all normal modes in each localized states; (iii) time integrals  $I_{B_1 A_\pm}$  for a given  $\omega$ ; and (iv) sum over all localized states and extended states  $\sum_{AB}$ . Although the result obtained in this way should be accurate and predictive, it is useful to develop an approximate theory, which also provides functional dependence of transport on various material parameters.

In this paper, we will first present a tractable model for the conductivity and Hall mobility in AS. Then, we will use this model to simplify the conductivity expressions obtained in the MRM for the three simplest transitions: LL, LE, and EL transitions driven solely by external field [cf. Figs. 2(a), 2(b), and 6(a) of [7]]. The conductivity from EE transition caused by disorder has been solved in the coherent potential approximation,<sup>13,14</sup> exhibits weak temperature dependence, and we will not consider it further.

The outline of the paper is as following. In Sec. II, we describe our approximation for the lattice vibrations and e-ph in coupling. In Sec. III A, we first illustrate that the MRM conductivity can be put in the customary form of relaxation time approximation and of Greenwood formula. At moderately high temperature, we invoke an asymptotic expansion to simplify the time integrals  $I_{B_1 A_\pm}$ . Under the approximations introduced in Sec. II, one can (i) obtain the velocity matrix elements analytically, and (ii) partially carry out the twofold summations over the initial and final electronic states. The conductivity from EL transitions is obtained in Sec. III B. The conductivity from LL transitions is calculated in Sec. III C. The matrix elements of electronic velocity could be carried out in a spherical coordinate system analytically. The conductivity from the LE transitions is the same order of magnitude as those from the LL transitions. Below a crossover temperature  $T^*$ , the later is larger; above  $T^*$ , the former is larger. This phenomenon is the main reason for the kink in the experimental  $\log_{10} \sigma$  versus  $1/T$  curve. As a demonstration, the numerical results for  $n$ -doped  $a$ -Si:H and  $a$ -Ge:H samples are given.

## II. APPROXIMATE IMPLEMENTATION OF MRM

### A. Vibrations

To calculate the e-ph interaction for a localized state, we need the transformation matrix between the atomic displacements and normal modes.<sup>6</sup> Because most amorphous materials are isotropic<sup>1,2</sup> and only acoustic modes are important for the e-ph interaction in one-component semiconductors,<sup>15</sup> one can use the acoustic dispersion relation for the vibrational spectrum:

$$\omega_{\mathbf{k}} = \bar{c}k, \quad k = |\mathbf{k}| \quad (5)$$

TABLE I. Parameters for vibrational spectrum.

	B (GPa)	$\mu$ (GPa)	$\bar{c}$ ( $10^3$ m/s)	$k_D$ ( $\text{\AA}^{-1}$ )	$\rho_m$ (g/cm <sup>3</sup> )
$a$ -Si (Refs. 12,16,17)	100	52	6.21	1.44	2.33
$a$ -Ge (Refs. 12,16,17)	75	41	3.08	1.38	5.33

where  $\omega_{\mathbf{k}}$  is the angular frequency for any mode characterized by wave vector  $\mathbf{k}$ . For every  $\mathbf{k}$ , there are one longitudinal and two transverse modes. We will use  $\mathbf{k}\tau$  to label a normal mode, where  $\tau = 1, 2, 3$  is the index of phonon branches.<sup>18</sup> Although translational invariance is destroyed in AS, standing wave modes are still well defined. Here,  $\bar{c}$  is the average speed of sound:

$$\frac{3}{\bar{c}^3} = \frac{2}{c_t^3} + \frac{1}{c_l^3}, \quad (6)$$

where  $c_t$  and  $c_l$  are the speeds of transverse and longitudinal waves, which are determined by<sup>18</sup> the bulk modulus  $B$  and shear modulus  $\mu$ . The cutoff wave vector  $k_D = (6\pi^2 n_a)^{1/3}$  is determined by the number density  $n_a = \mathcal{N}/V$  of atoms, where  $V$  is the volume of an AS and  $\mathcal{N}$  is total number of atoms.<sup>19</sup>  $n_a$  can be inferred from the observed mass density  $\rho_m$ . For  $a$ -Si and  $a$ -Ge,  $\rho_m$ ,  $B$ ,  $\mu$ ,<sup>9,12</sup>  $k_D$ , and  $\bar{c}$  are listed in Table I. For  $a$ -Si, the Debye frequency  $\omega_D$  is  $8.91 \times 10^{13}$  Hz, not far from the observed cutoff frequency<sup>20</sup>  $70 \text{ meV} = 1.07 \times 10^{14}$  Hz.

It is convenient to use  $\{x_{3(j-1)+1}, x_{3(j-1)+2}, x_{3(j-1)+3}\}$  to represent the vibrational displacement vector  $\mathbf{u}_j = \{u_{jx}, u_{jy}, u_{jz}\}$  for the  $j$ th atom ( $j = 1, 2, 3, \dots, \mathcal{N}$ ). Denote  $\Theta_\alpha$  ( $\alpha = 1, 2, \dots, 3\mathcal{N}$ ) as the normal coordinate of the  $\alpha$ th mode, so that the atomic displacements and the normal modes are related by

$$x_m = \sum_{\alpha} \Delta_{m\alpha} \Theta_{\alpha}, \quad m = 1, 2, \dots, 3\mathcal{N} \quad (7)$$

where  $\Delta$  is the minor of the determinant  $|\Lambda_{jl} - \omega^2 M_j \delta_{jl}|$  ( $j, l = 1, 2, 3, \dots, 3\mathcal{N}$ ), and  $\Lambda$  is the force constant matrix.<sup>21</sup> When we use  $\mathbf{k}\tau$  to label modes,  $\sum_{\alpha} \rightarrow \sum_{\mathbf{k}\tau}$ .

For a localized state, the shifts in the origins of normal modes caused by the e-ph interaction are the key quantities to determine the reorganization energy for the transitions involving the localized state.<sup>6</sup> The shift in origin is determined<sup>6</sup> by  $\Lambda^{-1}$ ,  $\Delta$ , and the e-ph coupling constant.  $\Lambda^{-1}$  and  $\Delta$  are complicated for a system with many atoms. To avoid using  $\Lambda^{-1}$  and find a more practical  $\Delta$ , we use a continuum to model the discrete random network of AS. In a continuum, one can classify the atomic vibrations according to possible standing wave modes. There is no reciprocal lattice for AS. Because a continuum is isotropic and has continuous translational symmetry, the wave vectors of the possible standing waves ( $\mathbf{k}$  points) are uniformly distributed in the wave-vector space (Debye sphere  $S_D$ ). The  $\mathcal{N}$   $\mathbf{k}$  points inside  $S_D$  correspond to  $3\mathcal{N}$  vibrational modes.

The atomic displacement  $\mathbf{u}$  at position  $\mathbf{R}$  and time  $t$  satisfies the wave equation

$$\frac{1}{\bar{c}^2} \frac{\partial^2 \mathbf{u}(\mathbf{R}, t)}{\partial t^2} = \nabla^2 \mathbf{u}(\mathbf{R}, t). \quad (8)$$

The plane-wave solution of Eq. (8) is<sup>19</sup>

$$\mathbf{u}(\mathbf{R}, t) = \frac{1}{\mathcal{N}^{1/2}} \sum_{\mathbf{k}\tau} e^{i\mathbf{k}\cdot\mathbf{R}} \mathbf{e}_{\mathbf{k}\tau} \Theta_{\mathbf{k}\tau} e^{-i(t\bar{c}\mathbf{k} + \varphi_{\mathbf{k}\tau})}, \quad (9)$$

where  $\mathbf{e}_{\mathbf{k}\tau}$  is the polarization vector of mode  $\mathbf{k}\tau$ . For a one-component system,<sup>19</sup>

$$\mathbf{e}_{\mathbf{k}\tau} \cdot \mathbf{e}_{\mathbf{k}\tau'}^* = \delta_{\tau\tau'}. \quad (10)$$

$\Theta_{\mathbf{k}\tau}$  and  $\varphi_{\mathbf{k}\tau}$  are the amplitude and phase of mode  $\mathbf{k}\tau$ , and are determined by the initial conditions. The inverse of Eq. (9) is

$$\Theta_{\mathbf{k}\tau} e^{-i(t\bar{c}\mathbf{k} + \varphi_{\mathbf{k}\tau})} = \frac{1}{\mathcal{N}^{1/2}} \sum_{\mathbf{R}} \mathbf{u}(\mathbf{R}, t) \cdot \mathbf{e}_{\mathbf{k}\tau}^* e^{-i\mathbf{k}\cdot\mathbf{R}}. \quad (11)$$

The normal coordinate of mode  $\mathbf{k}\tau$  is  $\Theta_{\mathbf{k}\tau} e^{-i(t\bar{c}\mathbf{k} + \varphi_{\mathbf{k}\tau})}$ , so that

$$\Delta_{\mathbf{u}(\mathbf{R}), \mathbf{k}\tau} = \mathcal{N}^{-1/2} e^{i\mathbf{k}\cdot\mathbf{R}} \mathbf{e}_{\mathbf{k}\tau} \quad (12)$$

and

$$(\Delta^{-1})_{\mathbf{k}\tau, \mathbf{u}(\mathbf{R})} = \mathcal{N}^{-1/2} e^{-i\mathbf{k}\cdot\mathbf{R}} \mathbf{e}_{\mathbf{k}\tau}^*. \quad (13)$$

In other words, the  $\mathbf{u}(\mathbf{R})$ th column of matrix  $\Delta^{-1}$  is the  $(\mathbf{k}\tau)$ th eigenvector that belongs to the  $(\mathbf{k}\tau)$ th eigenvalue  $(\omega_{\mathbf{k}\tau})^2 = (\bar{c}\mathbf{k})^2$  of the matrix of force constants. Equations (12) and (13) as consequences of Eq. (8) are contained in the Debye assumption (5).

### B. Localized states

To obtain analytical expressions for the e-ph interaction in a localized state and the velocity matrix elements, we need reasonable and simple approximate wave functions for localized and extended states. We assume all localized states are spherically symmetric. The difference among localized states is expressed by the localization length.<sup>2</sup> For a localized state  $A$ , denote  $\mathbf{R}_A$  as the position vector of the center, and the normalized wave function is

$$\phi_A(\mathbf{r} - \mathbf{R}_A) = \pi^{-1/2} \xi_A^{-3/2} e^{-|\mathbf{r} - \mathbf{R}_A|/\xi_A}, \quad (14)$$

where  $\mathbf{r}$  and  $\xi_A$  are the coordinate of electron and localization length.<sup>22</sup> Following Mott,  $\xi_A$  is determined by the eigenvalue  $E$  of localized state  $\phi_A$  (Ref. 22):

$$\xi_E = \frac{bZe^2}{4\pi\epsilon_0\epsilon}(E_c - E)^{-1}, \quad (15)$$

where  $Z$  is the effective nuclear charge of an atom core and  $\epsilon$  is the static dielectric constant.  $E_c$  is the mobility edge and  $b$  is a dimensionless constant.  $b$  is determined by the shortest possible localization length  $\xi_{\min}$  with  $E = 0$ . Realistic calculations of tail states are given in Refs. 23–27.

The parameters<sup>1,12</sup> for electron-core interaction and localized state are listed in Table II. In  $a$ -Si:H and  $a$ -Ge:H,<sup>1,12</sup> the most localized states are associated with dangling bonds. The localization length is one half the average bond length:  $\xi_{\min} = 2.35 \text{ \AA}/2$  and  $2.45 \text{ \AA}/2$ . Using Eq. (15), one has  $b = 0.121$  and  $0.170$ . The measured value of mobility edge for  $a$ -Si is rather dispersed:<sup>28,29</sup> 0.2–2 eV; we will take<sup>30</sup>  $E_c = 0.5 \text{ eV}$ . Figure 1 plots localization length versus eigenenergy, and we purposely left out a small neighborhood ( $E_c - U, E_c$ ) of  $E$ , where  $U$  is the Urbach energy for band tail. When  $\xi_E$  is larger than the linear size of a physical infinitesimal volume

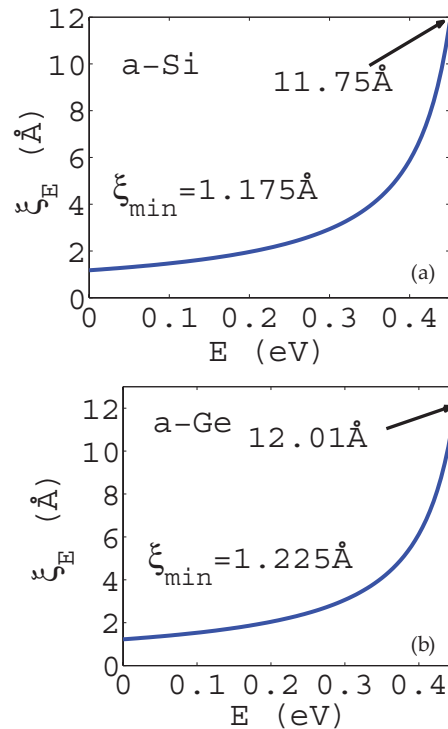


FIG. 1. (Color online) Localization length as function of energy: (a)  $a$ -Si, (b)  $a$ -Ge.

element<sup>16</sup> ( $\sim 100 \text{ \AA}$ ), the corresponding localized state acts like an extended state for purposes of transport.

There is a distinction between a large polaron and a carrier in a weakly localized state with  $\xi$  several tens of  $\text{\AA}$ . A large polaron can move freely before meeting a scatterer, while a localized carrier in AS is trapped in the region where  $\phi_A$  has support. To make a localized carrier move, thermal activation involving a reorganization of vibrational configuration is necessary.<sup>6</sup>

Because (i) no translational invariance exists in an AS and (ii) a localized electronic state is confined in some finite region, the spatial distribution of localized states needs special attention. For various macroscopic properties, an AS can be viewed as isotropic and uniform at a length scale larger than<sup>16</sup> 10 nm (this effectively defines the physical infinitesimal volume element  $\Omega$ ). Therefore, it is convenient to describe the spatial distribution of localized states in a spherical coordinate system. For a given origin and polar axis, the sum over localized states  $A_1$  can be changed into an integral over a combined spatial and energetic distribution of localized states:

$$\sum_{A_1} \rightarrow \int_0^{R_c} R^2 dR \int_0^\pi \sin\theta d\theta \int_0^{2\pi} d\phi \int_{-\infty}^{E_c} dE f(R, \theta, \phi; E), \quad (16)$$

where  $R$  is the distance between the origin and the center  $\mathbf{R}_{A_1}$  of a localized state  $\phi_{A_1}$ ,  $R_c$  is the radius of an AS sample,  $f(R, \theta, \phi; E)$  is the number of localized states in a volume element defined by  $(R, R + dR)$ ,  $(\theta, \theta + d\theta)$ , and  $(\phi, \phi + d\phi)$  with energy  $(E, E + dE)$ , i.e., position-dependent density of states. Since a volume element with a linear size of 10 nm is representative for an AS, in the calculation of transport

TABLE II. Parameters for electronic state.

	$E_c$ (eV)	$U$ (meV)	$n_{\text{loc}}$ ( $\text{\AA}^{-3}$ )	$Z$	$\epsilon$	$q_{\text{TF}}$ ( $\text{\AA}^{-1}$ )	$b$
$a$ -Si	0.5 (Ref. 30)	50 (Ref. 31)	$5/10.86^3$ (Ref. 32)	4	11.68	1.7	0.121
$a$ -Ge	0.5	51	$5/11.32^3$	4	16	1.7	0.170

coefficients, one may replace the volume  $V$  of the entire AS sample with the volume  $\Omega$  of a physical infinitesimal volume element. Then,  $R_c$  is the radius of  $\Omega$ .

In a physical infinitesimal volume  $\Omega$ , various possible atomic configurations appear according to the proper statistical weights, which would be found in a much larger sample. Therefore, the coarse-grained average  $\bar{f}$  of  $f(R, \theta, \phi; E)$  over such a physical infinitesimal volume element is no longer position dependent:  $\bar{f} = N(E)$ , where  $N(E)$  is the usual density of states. However, the weight factors in Eq. (16) play an important role in determining transport properties. The reason is that although  $\bar{f}$  is independent of  $(R, \theta, \phi)$ , the transition amplitudes (velocity matrix elements) depend on the relative position of another localized state or on the wave-vector direction of the involved extended state.

For many AS,<sup>33,34</sup> in the range of band tail, the density of localized states satisfies

$$\bar{f}(R, \theta, \phi; E) = N(E) = \frac{n_{\text{loc}}}{U} e^{-(E_c - E)/U}, \quad (17)$$

where  $U$  is the Urbach energy and  $n_{\text{loc}}$  is the number of localized states per unit volume. The pre-exponential factor is determined from the requirement that the integral of  $N(E)$  over all localized energy spectrum should be  $n_{\text{loc}}$ . In general,  $E_c$  and  $U$  take different values for the valence band and the conduction band.<sup>34</sup> Denote  $n$  as the carrier concentration, and the Fermi energy  $E_F$  of a weakly doped AS is

$$E_F = E_c + U \ln(n/2n_{\text{loc}}). \quad (18)$$

When  $n \leq 2n_{\text{loc}}$ , all occupied states are localized at  $T = 0$  K. For  $a$ -Si, the conduction-band energy spectrum (17) is illustrated in Fig. 2. We can see from Fig. 1(a) and Eq. (17) that most localized states in  $a$ -Si have a localization length in the range 6–12  $\text{\AA}$ . In approximation (17), the density of states  $N(E)$  of localized states reaches its maximum at

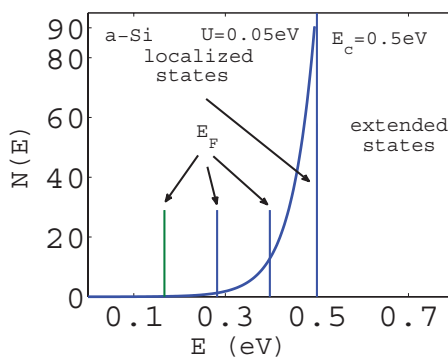


FIG. 2. (Color online) Density of states of the conduction tail for  $n$ -doped  $a$ -Si samples: the first three vertical lines are the Fermi energy for  $n = 10^{19}$ ,  $10^{20}$ , and  $10^{21}$   $\text{cm}^{-3}$ . The rightmost vertical line is the mobility edge.

$E_c$ . Therefore, the most probable localization length is  $\bar{\xi} = cZe^2/(4\pi\epsilon_0\epsilon U)$ . For  $a$ -Si,  $\bar{\xi} = 11.75$   $\text{\AA}$ . This is consistent with various experiments.<sup>35–41</sup>

Making use of relation (15), the integral over the energy eigenvalues of localized states is converted into an integral over localization lengths:

$$\int_{-\infty}^{E_c} dE_A N(E_A) \rightarrow \frac{bZe^2 n_{\text{loc}}}{4\pi\epsilon_0\epsilon U} \int_0^{\infty} \frac{d\xi}{\xi^2} \exp\left(-\frac{bZe^2}{4\pi\epsilon_0\epsilon U\xi}\right). \quad (19)$$

Comparing Eq. (16) with the sum over states  $\sum_{\mathbf{k}} \rightarrow \int_{\text{BZ}} \frac{V d^3k}{(2\pi)^3}$  in a crystal is helpful, where  $\mathbf{k}$  is the wave vector of a Bloch state in Brillouin zone, and  $V$  is volume of the crystal. The matrix elements behind  $\sum_{\mathbf{k}}$  may depend on the direction of  $\mathbf{k}$ ,  $d^3k = k^2 dk \sin\theta_k d\theta_k d\phi_k$  takes into account the dependence on the two wave vectors of two Bloch states.

### C. Extended states

If one imagines that an AS is obtained from deforming its reference crystal, an extended state in the AS can be viewed as a superposition of a principal Bloch wave with a given wave vector and its scattered secondary waves.<sup>42,43</sup> The scattered waves are produced by scattering the principal Bloch wave with the disorder potential (the difference between the potential energy in the AS and that in its reference crystal).<sup>42,43</sup> Excepting the EE transitions driven by external field, we may approximate an extended state  $\chi_{B_1}(\mathbf{r})$  by a plane wave with certain momentum  $\mathbf{p}$ , and its eigenenergy is that of the plane wave:

$$\chi_{B_1} = V^{-1/2} e^{i\mathbf{p}\cdot\mathbf{r}/\hbar}, \quad E_{B_1} = p^2/2m, \quad (20)$$

where  $V$  is the volume of AS sample, and the energy zero point of extended states is at the mobility edge  $E_c$ . An extended state in an AS is labeled by the wave vector of its principal Bloch wave. The sum over extended states becomes an integral over momentum:  $\sum_{B_1} \rightarrow \int \frac{V d^3p}{(2\pi\hbar)^3}$ .

### D. Interaction between a carrier and an atomic core

In a solid, the attraction to an electron from an atomic core may be crudely approximated by a screened Coulomb potential<sup>19</sup>

$$V(\mathbf{r}) = \frac{Ze^2}{4\pi\epsilon_0\epsilon} \frac{e^{-q_{\text{TF}}r}}{r}, \quad (21)$$

where  $\mathbf{r}$  is the position of electron relative to an atomic core.  $q_{\text{TF}} = 2.95(r_s/a_0)^{-1/2} \text{\AA}^{-1}$  is the Thomas-Fermi wave vector, and is determined by the carrier density.  $r_s/a_0$  is a number about 2 to 6. For  $a$ -Si:H (Ref. 1) and  $a$ -Ge,<sup>12</sup> we take the value for  $c$ -Si and  $c$ -Ge:  $q_{\text{TF}} = 1.7 \text{\AA}^{-1}$ .

### E. Electron-phonon coupling in a localized state

We consider the mean e-ph interaction in a localized state  $\phi_A$ . The e-ph interaction Hamiltonian is

$$H_{e\text{-ph}} = \sum_{n\sigma} u_{n\sigma} \frac{\partial V(\mathbf{r} - \mathbf{R}_n)}{\partial X_{n\sigma}}, \quad \sigma = x, y, z \quad (22)$$

where  $\mathbf{R}_n$  ( $X_{nx}, X_{ny}, X_{nz}$ ) is the position vector of the  $n$ th atom, and  $u_{n\sigma}$  is the  $\sigma$ th Cartesian component of vibrational amplitude of the  $n$ th atom. Usually, the average e-ph interaction in state  $\phi_A$  is written in a linear coupling form<sup>44</sup>

$$\int d^3x \phi_A^*(\mathbf{r} - \mathbf{R}_A) H_{e\text{-ph}} \phi_A(\mathbf{r} - \mathbf{R}_A) = - \sum_{n\sigma} u_{n\sigma} g_{n\sigma}^A, \quad (23)$$

where  $g_{n\sigma}^A$  is the e-ph coupling constant in state  $\phi_A$ . Because we consider only localized state  $\phi_A$ , it is convenient to shift the origin of coordinate to the center  $\mathbf{R}_A$  of  $\phi_A$ . In Eq. (22), we sum over all the atoms in  $V$  of an AS sample. In addition, the factors  $V(\mathbf{r} - \mathbf{R}_n)$  and  $\phi_A(\mathbf{r} - \mathbf{R}_A)$  in the integrand of Eq. (23) involve two atoms, and directly integrating over coordinate is difficult (requiring ellipsoidal coordinate system). To obtain the coupling constant  $g_{n\sigma}^A$ , we Fourier transform  $\partial V(\mathbf{r} - \mathbf{R}_n)/\partial X_{n\sigma}$  in the left-hand side of Eq. (23), first carry out the integral in coordinate  $\mathbf{r}$ , then execute the integral over wave vector  $\mathbf{q}$ . The final result is

$$g_{n\sigma}^A = \frac{16(Ze^2/4\pi\epsilon_0\epsilon) X_{n\sigma}}{\xi^4} \left\{ \frac{R_n}{R_n^2} \frac{e^{-2R_n/\xi}}{2 q_{\text{TF}}^2 - (2/\xi)^2} + \left[ \frac{q_{\text{TF}} e^{-q_{\text{TF}} R_n} - (2/\xi) e^{-2R_n/\xi}}{[(2/\xi)^2 - q_{\text{TF}}^2]^2} - \frac{\xi}{8} \frac{e^{-2R_n/\xi}}{q_{\text{TF}}^2 - (2/\xi)^2} \right] + \frac{1}{R_n} \left[ \frac{e^{-q_{\text{TF}} R_n} - e^{-2R_n/\xi}}{[(2/\xi)^2 - q_{\text{TF}}^2]^2} - \frac{\xi^2}{16} \frac{e^{-2R_n/\xi}}{q_{\text{TF}}^2 - (2/\xi)^2} \right] \right\}, \quad (24)$$

where  $R_n = |\mathbf{R}_n - \mathbf{R}_A|$  is the distance between the  $n$ th atom to the center  $\mathbf{R}_A$  of localized state  $\phi_A$ . The first term decays exponentially, and the second and the third terms contain additional decay factors  $R_n^{-1}$  and  $R_n^{-2}$ , respectively. Since we are concerned only with localized state  $\phi_A$ , hereafter we drop the subscript  $A$  on  $\xi$  and  $g$ .

### F. Polaron formation

The static displacements of atoms induced by the e-ph interaction measure the strength of e-ph interaction and determine whether the e-ph coupling should be treated as a perturbation or be included in the zeroth-order Hamiltonian.<sup>6</sup> The static displacement of the  $m$ th atomic degree of freedom caused by the e-ph interaction in localized state  $\phi_A$  is<sup>6</sup>

$$x_m^{A0} = \sum_p (\Lambda^{-1})_{mp} g_p^A, \quad m, p = 1, 2, \dots, 3\mathcal{N} \quad (25)$$

where  $\Lambda^{-1}$  is the inverse of force constant matrix. The shift  $\Theta_\alpha^A$  in origin of the  $\alpha$ th ( $\alpha = 1, 2, \dots, 3\mathcal{N}$ ) mode by the carrier localized in state  $\phi_A$  is<sup>6</sup>

$$\Theta_\alpha^A = \sum_m (\Delta^{-1})_{\alpha m} x_m^{A0}. \quad (26)$$

This has the physical interpretation of the polaronic relaxation due to the e-ph coupling.

If  $\Lambda^{-1}$  and  $\Delta^{-1}$  were known analytically, we could use Eq. (25) to find  $\{x_m^{A0}\}$ , and then use Eq. (26) to find  $\{\Theta_\alpha^A\}$ . The continuum model in Sec. II A allows us to first find the shifts in origins  $\{\Theta_\alpha^A\}$  of normal modes in a localized state. Then, static displacements  $\{x_m^{A0}\}$  can be obtained from Eq. (7). In the continuum model, the normal modes are labeled by wave vectors  $\mathbf{k}$ . By substituting Eq. (25) into Eq. (26), and noticing  $\Delta^{-1} \Lambda^{-1} = W^{-1} \Delta^T$ , where  $(W^{-1})_{\alpha\beta} = \delta_{\alpha\beta} M_\alpha^{-1} \omega_\alpha^{-2}$ , one concludes that

$$\Theta_{\mathbf{k}\tau}^A = M_{\mathbf{k}}^{-1} \omega_{\mathbf{k}}^{-2} \sum_{n\sigma} g_{n\sigma}^A \Delta_{n\sigma, \mathbf{k}\tau}, \quad (27)$$

where  $n = 1, 2, 3, \dots, \mathcal{N}$  and  $\sigma = x, y, z$ . Substituting Eq. (12) into Eq. (27) and replacing the sum by an integral over all space, Eq. (27) becomes

$$\Theta_{\mathbf{k}\tau}^A = \frac{\text{Re} \sum_\sigma \int_V d^3X g_{\mathbf{R}\sigma}^A e_{\mathbf{k}\tau}^\sigma e^{i\mathbf{k}\cdot\mathbf{R}}}{\mathcal{N}^{1/2} M_{\mathbf{k}} \omega_{\mathbf{k}}^2 \Omega_a}, \quad (28)$$

where  $\Omega_a = V/\mathcal{N}$  is the average volume occupied by one atom. For  $a$ -Si and  $a$ -Ge,<sup>12,19</sup>  $\Omega_a \approx (5.43 \text{ \AA})^3/4$  and  $(5.66 \text{ \AA})^3/4$ . Equation (28) expresses the shift  $\Theta_{\mathbf{k}}^A$  in the origin of normal mode  $\mathbf{k}$  with the e-ph coupling constant  $g_{n\sigma}^A$ . We take  $\mathbf{k}$  as the polar axis ( $z$  axis) and transform to a spherical coordinate system because the integrand of Eq. (28) does not contain azimuthal angle  $\phi$ , and  $\{g_{nx}^A\}$  and  $\{g_{ny}^A\}$  do not contribute to  $\Theta_{\mathbf{k}\tau}^A$ . Only when  $g_{nz}^A$  has a component along  $\mathbf{k}$  does it contribute to  $\Theta_{\mathbf{k}\tau}^A$ . The integrations over the  $R^{-2}$  and  $R^{-3}$  terms in Eq. (24) are purely imaginary, and do not contribute to  $\Theta_{\mathbf{k}}^A$ . The origin shift of mode  $\mathbf{k}\tau$  induced by the e-ph interaction in localized state  $\phi_A$  is

$$\Theta_{\mathbf{k}\tau}^A = \frac{1}{\mathcal{N}^{1/2} M_{\mathbf{k}} k^2 \bar{c}^2} \frac{2^7 \pi Z e^2 / (4\pi \epsilon_0 \epsilon \Omega_a \xi^5)}{[q_{\text{TF}}^2 - (2/\xi)^2][(2/\xi)^2 + k^2]^2}. \quad (29)$$

Because we take AS to be an isotropic continuous medium,  $\Theta_{\mathbf{k}\tau}^A$  depends only on the magnitude  $k$ . The  $k^{-2}$  divergence in Eq. (29) when  $k \rightarrow 0$  is caused by the Debye spectrum ( $\omega_{\mathbf{k}} = \bar{c}k$ ). In a Debye model, the number of modes per unit volume per unit angular frequency interval is<sup>19</sup>  $(2\pi^2 \bar{c})^{-1} 3k^2$  when  $k < k_D$ . The shift is smaller for higher wave number, and decays with wave vector  $\mathbf{k}$  as  $[(2/\xi)^2 + k^2]^{-2}$ . Because for all materials<sup>19</sup>  $q_{\text{TF}} \sim 1.2\text{--}2.1 \text{ \AA}^{-1}$ , while  $\xi > 2 \text{ \AA}$  for localized states caused by topological disorder,<sup>22</sup> the factor  $[q_{\text{TF}}^2 - (2/\xi)^2]$  in the denominator of Eqs. (24), (29), (31), (34), and (37) will not lead to a divergent result.

Equation (29) exhibits two obvious features: (i)  $\Theta_{\mathbf{k}}^A > 0$  for every mode  $\mathbf{k}$ ; (ii) if  $\xi_{A_1} < \xi_{A_2}$ , then  $\Theta_{\mathbf{k}}^{A_1} > \Theta_{\mathbf{k}}^{A_2}$  for every mode  $\mathbf{k}$ . We have shown that three-state conduction processes, which are first order in residual interactions, are the same order of magnitude as the two-state processes discussed here.<sup>7</sup> Also, in the lowest-order self-consistent approximation, three- and four-state processes must be included in the Hall mobility calculation.<sup>7</sup> Some of the aforementioned transport processes involve at least two localized states. To carry out asymptotic expansion at high temperature for such processes, the features (i) and (ii) are essential.

The static atomic displacements in localized state  $A$  can be found from Eqs. (26) and (29):

$$x_{\sigma}^{0A}(\mathbf{R}) = \frac{\mathcal{N}^{1/2} \Omega_a}{(2\pi)^3} \sum_{\tau=1}^3 \int d^3k e^{i\mathbf{k}\cdot\mathbf{R}} \Theta_{\mathbf{k}\tau}^A e_{\mathbf{k}\tau}^{\sigma}. \quad (30)$$

Next, substitute Eq. (29) into Eq. (30) and carry out the integral. One finds the displacement  $x^{0A}$  along the radial direction for an atom at  $\mathbf{R}$  caused by e-ph interaction in a localized state:

$$x^{0A}(\mathbf{R}) = \frac{4}{M\bar{c}^2} \frac{Z^* e^2 / 4\pi\epsilon_0\epsilon}{\xi [q_{\text{TF}}^2 - (2/\xi)^2]} \frac{1 - \frac{1}{2}e^{-2R/\xi}}{R}, \quad (31)$$

where we have let  $k_D \rightarrow \infty$  to obtain an analytic result. It is interesting to notice that Eq. (31) is similar to the wave function of large polaron in the strong-coupling limit (cf. Ref. 15).

Figure 3(a) is an illustration of Eq. (31) for  $a$ -Si at  $\xi = 11.75$  and  $23.50$  Å (5 and 10 times bond length). We observe that the more localized (smaller  $\xi$ ) the state, the larger the atomic displacements, i.e., the stronger e-ph interaction (larger atomic displacements). This agrees with previous experiments and simulations.<sup>45,46</sup> For the hardest mode<sup>20</sup>  $\omega = 70$  meV of  $a$ -Si, the amplitude  $A_0 = (\hbar/M\omega)^{1/2}$  of zero-point vibration is  $0.046$  Å, and the amplitude  $A_{th} = (k_B T/M\omega^2)^{1/2}$  of thermal vibration at 300 K is  $0.028$  Å. Considering these two peaks of the  $a$ -Si phonon spectrum are at<sup>20</sup> 20 meV ( $A_0 = 0.086$  Å,  $A_{th} = 0.098$  Å) and 60 meV ( $A_0 = 0.050$  Å,  $A_{th} = 0.033$  Å), the static displacements of atoms estimated in Eq. (31) are twice the amplitude of vibrations. Comparing the root mean square of bond-length fluctuation  $0.2$  Å (geometric

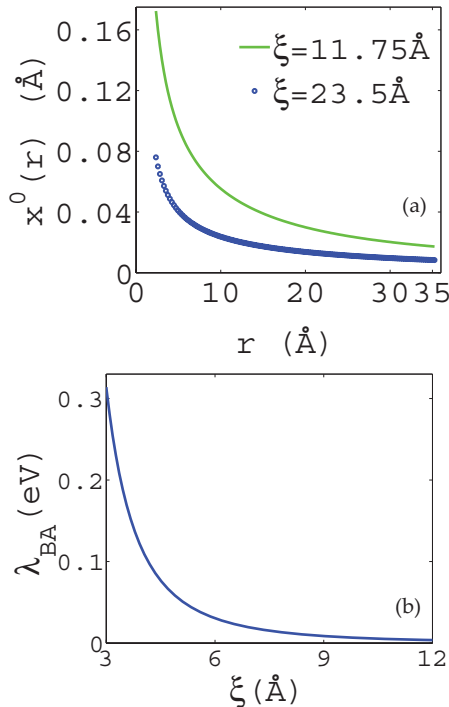


FIG. 3. (Color online) (a) Static displacements  $x^0(\mathbf{r})$  of atoms in a localized state  $\phi_A$  as function of the distance  $r$  to the center of  $\phi_A$  in  $a$ -Si: solid line is for  $\xi = 11.75$  Å, circle line is for  $\xi = 23.5$  Å. The displacements are larger in a more localized state. (b) The binding energy caused by e-ph interaction as a function of localization length. The binding energy is larger for a more localized state.

disorder) from *ab initio* molecular dynamics simulation,<sup>23</sup> the approximate acoustic dispersion relation (5) somewhat overestimates the long-wave contribution in Eqs. (28), (29), (30), and (31).

### G. Reorganization energy

Unlike a carrier in an extended state, a carrier in a localized state is confined by the disorder potential. Beyond that, the e-ph interaction produces<sup>6</sup> an additional binding energy  $E_b^A$  to a localized carrier in  $\phi_A$ :

$$E_b^A = \frac{1}{2} \sum_{\alpha} M_{\alpha} \omega_{\alpha}^2 (\Theta_{\alpha}^A)^2. \quad (32)$$

Because the reorganization energy measures the energy shift from initial vibrational configuration to the final vibrational configuration,  $E_b^A$  is the same as<sup>6</sup> the reorganization energy  $\lambda_{BA}$  of LE transition  $\phi_A \rightarrow \chi_B$  and the reorganization energy  $\lambda_{AB}$  of EL transition  $\chi_B \rightarrow \phi_A$ :  $\lambda_{AB} = \lambda_{BA} = E_b^A$ . For the continuous medium model, the sum over modes in Eq. (32) may be converted to an integral over the Debye sphere in spherical coordinate system  $(k, \theta', \phi')$ :

$$\lambda_{AB} = \frac{\mathcal{N} \Omega_a}{2(2\pi)^3} \sum_{\tau=1}^3 \int_0^{k_D} dk k^2 \times \int_0^{\pi} d\theta' \sin \theta' \int_0^{2\pi} d\phi' M k^2 \bar{c}^2 (\Theta_{\mathbf{k}\tau}^A)^2. \quad (33)$$

Owing to spherical symmetry in Eq. (33), the direction of polar axis is arbitrary. Substituting Eq. (29) into (33) and carrying out the integral, one finds

$$\lambda_{AB} = 2\pi \frac{(2^7 \pi Z^* e^2 / 4\pi\epsilon_0\epsilon)^2 \xi}{2^7 M \bar{c}^2 \Omega_a [(\xi q_{\text{TF}})^2 - 4]^2} \left( \frac{15}{48} \tan^{-1} \frac{k_D \xi}{2} + \frac{k_D \xi [1 + (\frac{k_D \xi}{2})^2]^{-1} \left\{ \left[ 1 + \left( \frac{k_D \xi}{2} \right)^2 \right]^{-2} + \frac{5}{4} \left[ 1 + \left( \frac{k_D \xi}{2} \right)^2 \right]^{-1} + \frac{15}{8} \right\}}{12} \right). \quad (34)$$

Figure 3(b) displays the change in binding energy with localization length. We can see that more localized states have larger binding energy. In other words, when a carrier leaves or enters a more localized state, the required reorganization energy is larger, and the corresponding LE and EL transitions are more hindered.

The reorganization energy  $\lambda_{A_2 A_1}$  for LL transition  $\phi_{A_1} \rightarrow \phi_{A_2}$  satisfies a reciprocity condition<sup>6</sup>  $\lambda_{A_1 A_2} = \lambda_{A_2 A_1}$ , where

$$\lambda_{A_2 A_1} = \frac{1}{2} \sum_{\alpha} M_{\alpha} \omega_{\alpha}^2 (\Theta_{\alpha}^{A_2} - \Theta_{\alpha}^{A_1})^2. \quad (35)$$

Equation (35) can be expressed as

$$\lambda_{A_2 A_1} = |E_b^{A_1}| + |E_b^{A_2}| - B_{A_2 A_1}, \quad (36)$$

where  $E_b^{A_1}$  is obtained from Eq. (34) by replacing  $\xi$  with  $\xi_1$ ,  $\xi_1$  is the localization length of  $\phi_{A_1}$ .  $B_{A_2 A_1} = \sum_{\alpha} \hbar \omega_{\alpha} \theta_{\alpha}^{A_2} \theta_{\alpha}^{A_1}$  is

the interference term

$$B_{A_2A_1} = \frac{2^7 \pi Z^* e^2 / 4\pi \epsilon_0 \epsilon}{\Omega_a \xi_1^5 [q_{\text{TF}}^2 - (2/\xi_1)^2]} \frac{2^7 \pi Z^* e^2 / 4\pi \epsilon_0 \epsilon}{\xi_2^5 [q_{\text{TF}}^2 - (2/\xi_2)^2]} \frac{4\pi}{M c^2} \left\{ [(2/\xi_2)^2 - (2/\xi_1)^2]^{-2} \left[ \frac{\xi_1^3}{16} \tan^{-1} \frac{k_D \xi_1}{2} + \frac{k_D \xi_1^4}{8(k_D^2 \xi_1^2 + 4)} \right. \right. \\ \left. \left. + \frac{\xi_2^3}{16} \tan^{-1} \frac{k_D \xi_2}{2} + \frac{k_D \xi_2^4}{8(k_D^2 \xi_2^2 + 4)} \right] - 2[(2/\xi_2)^2 - (2/\xi_1)^2]^{-3} \left[ \frac{\xi_1}{2} \tan^{-1} \frac{k_D \xi_1}{2} - \frac{\xi_2}{2} \tan^{-1} \frac{k_D \xi_2}{2} \right] \right\}. \quad (37)$$

Equations (34), (36), and (37) determined the reorganization energy  $\lambda_{A_2A_1}$  for LL transition  $\phi_{A_1} \rightarrow \phi_{A_2}$ .

### III. CONDUCTIVITY FROM LE AND EL TRANSITIONS DRIVEN SOLELY BY FIELD

In this section, we assemble the approximations of the preceding section to estimate the various contributions to the conductivity.

#### A. LE transitions driven by field

##### 1. Connection to relaxation time approximation and Kubo-Greenwood formula

Inside the summation of Eq. (1), only electronic degrees of freedom appear. Each term can be written as

$$\begin{cases} \text{Re} \\ \text{Im} \end{cases} \sigma_{\alpha\beta}^{BA}(\omega) = (m_{\text{eff}}^{BA})_{\alpha\beta}^{-1} n e^2 \tau_{\pm}^{BA}(\omega), \quad (38)$$

where  $n = N_e / \Omega_s$  is the carrier density,

$$\tau_{\pm}^{BA}(\omega) = \text{Im } i [I_{BA+} \pm I_{BA-}]$$

may be viewed as a relaxation time for which the real part of conductivity takes plus sign, and the imaginary part takes the minus sign. Here,

$$(m_{\text{eff}}^{BA})_{\alpha\beta}^{-1} = - \frac{(w_{AB}^{\alpha} - v_{BA}^{\alpha})(v_{BA}^{\beta})^*}{2(E_A^0 - E_B^0)} \quad (39)$$

may be interpreted as the inverse of the effective mass tensor for transition  $\phi_A \rightarrow \chi_B$ . In this sense,  $\sigma_{\alpha\beta}^{B_1A}(\omega)$  is a generalization of the energy-dependent conductivity<sup>2</sup>  $\sigma_{\alpha\beta}^E(\omega)$ . With this notation, Eq. (1) becomes

$$\sigma_{\alpha\beta}(\omega) = \sum_{AB_1} \sigma_{\alpha\beta}^{B_1A}(\omega) [1 - f(E_{B_1})] f(E_A), \quad (40)$$

a generalization of the Kubo-Greenwood formula (2.11) of Refs. 2 and 49. This shows how a kinetic approach may be properly generalized to AS.

##### 2. High-temperature approximation of the time integral $I_{BA\pm}$

To calculate  $I_{BA\pm}(\omega)$  defined by Eq. (4), we change the integration variable from  $s$  to  $t$ :  $s = t - i\beta\hbar/2$ . Equation (4)

becomes

$$I_{BA\pm}(\omega) = \exp \left\{ -\frac{1}{2} \sum_{\alpha} \coth \frac{\beta\hbar\omega_{\alpha}}{2} (\theta_{\alpha}^A)^2 \right\} e^{\beta\hbar(\pm\omega + \omega_{AB})/2} \\ \times \int_{-\infty + i\beta\hbar/2}^{i\beta\hbar/2} dt e^{it(\pm\omega + \omega_{AB})} \\ \times \exp \left\{ \frac{1}{2} \sum_{\alpha} (\theta_{\alpha}^A)^2 \csc h \frac{\beta\hbar\omega_{\alpha}}{2} \cos t\omega_{\alpha} \right\}. \quad (41)$$

If we view  $t$  as a complex variable, the saddle point of  $\frac{1}{2} \sum_{\alpha} (\theta_{\alpha}^A)^2 \csc h \frac{\beta\hbar\omega_{\alpha}}{2} \cos t\omega_{\alpha}$  is at  $(0,0)$ . Because the integrand in Eq. (41) is analytic in the whole complex- $t$  plane, we can deform the integral path from  $(-\infty + i\beta\hbar/2, 0 + i\beta\hbar/2)$  to a new path  $C_1 + C_2 + C_3$  crossing the saddle point  $(0,0)$ , where  $C_1$ :  $(-\infty + i\beta\hbar/2, -\infty + i0]$ ,  $C_2$ :  $(-\infty, 0]$ ,  $C_3$ :  $(0 + i0, 0 + i\beta\hbar/2]$ . Because of the external field and residual interactions being adiabatically introduced,<sup>7</sup> the integration along  $C_1$  is zero. When  $k_B T \geq \hbar\bar{\omega}$  ( $\bar{\omega}$  is the frequency of the first peak in phonon spectrum),  $\sum_{\alpha} (\theta_{\alpha}^A)^2 k_B T / \hbar\bar{\omega}$  is large. The integrals along  $C_2$  and  $C_3$  can be asymptotically calculated by the Laplace method.<sup>50</sup> The final result for  $I_{BA\pm}$  is

$$I_{BA\pm}(\omega) = i\hbar/\lambda_{BA} + \frac{\hbar e^{\beta\hbar(\pm\omega + \omega_{AB})/2 - \gamma_{\pm}^{BA} - \lambda_{BA}/4k_B T}}{(k_B T \lambda_{BA})^{1/2}} \\ \times \left[ \frac{\sqrt{\pi}}{2} - iG(y_{\pm}^{BA}) \right], \quad (42)$$

where

$$y_{\pm}^{BA} = \frac{[\hbar(\pm\omega + \omega_{AB})]^2}{4\lambda_{BA} k_B T}, \quad \lambda_{BA} = \frac{1}{2} \sum_{\alpha} \hbar\omega_{\alpha} (\theta_{\alpha}^A)^2, \quad (43)$$

and

$$G(y_{\pm}) = \begin{cases} \sum_{n=0}^{\infty} \frac{y_{\pm}^{n+1/2}}{n!(2n+1)} & \text{if } y_{\pm} \leq 1, \\ \frac{e^{y_{\pm}}}{2\sqrt{y_{\pm}}} \left[ 1 + \sum_{n=1}^{\infty} \frac{(2n-1)!!}{2^n y_{\pm}^n} \right] & \text{if } y_{\pm} > 1. \end{cases} \quad (44)$$

The applicable condition for  $a$ -Si is  $T > 232$  K;<sup>20,51,52</sup> for  $a$ -Ge it is  $T > 115$  K.<sup>51-53</sup>

### 3. Velocity matrix elements

Under the approximations in Secs. II B and II C, the velocity matrix elements in Eq. (2) can be obtained by changing the integration variable from  $\mathbf{r}$  to  $\mathbf{r}' = \mathbf{r} - \mathbf{R}_A$ , and introducing a spherical coordinate system with  $\mathbf{R}_A$  as the origin and  $\mathbf{p}$  as polar axis. One can show that  $v_{B_1A}^x = v_{B_1A}^y = 0$ , i.e., for the velocity components perpendicular to  $\mathbf{p}$ , the matrix elements

are zero:

$$v_{\perp}^{B_1 A} = 0. \quad (45)$$

The matrix element of  $v^z$  (the velocity component parallel to  $\mathbf{p}$ ) is

$$v_{\parallel}^{B_1 A} = v_{B_1 A}^z = \frac{p}{m} 8\pi^{1/2} \frac{e^{-i\mathbf{p}\cdot\mathbf{R}_A/\hbar} V^{-1/2} \xi^{3/2}}{(1 + p^2 \xi^2/\hbar^2)^2}. \quad (46)$$

Similarly,

$$w_{\parallel}^{AB_1} = w_{AB_1}^z = -\frac{p}{m} 8\pi^{1/2} \frac{e^{-i\mathbf{p}\cdot\mathbf{R}_A/\hbar} V^{-1/2} \xi^{3/2}}{(1 + p^2 \xi^2/\hbar^2)^2}. \quad (47)$$

By substituting Eqs. (46) and (47) into (39), the inverse of the effective mass tensor becomes

$$(m_{\text{eff}}^{B_1 A^{-1}})_{\alpha\beta} = \frac{m^{-1} p_{\alpha} p_{\beta}}{m(E_{B_1}^0 - E_A^0)} \frac{32\pi \xi^3 V^{-1}}{(1 + p^2 \xi^2/\hbar^2)^4}. \quad (48)$$

Since for each Cartesian component<sup>2</sup>

$$\langle \chi_B | x_{\alpha} | \phi_A \rangle = \frac{i\hbar \langle \chi_B | v_{\alpha} | \phi_A \rangle}{(E_A - E_B)}, \quad \alpha = x, y, z, \quad (49)$$

from (45) and (46), one has

$$\langle \chi_B | r_{\perp} | \phi_A \rangle = 0 \quad \text{and} \quad \langle \chi_B | r_{\parallel} | \phi_A \rangle = \frac{i\hbar v_{\parallel}^{BA}}{(E_A - E_B)}. \quad (50)$$

#### 4. Relation to kinetic method

Because  $\phi_A$  vanishes at  $x_{\alpha} = \pm\infty$  ( $\alpha = x, y, z$ ), by means of partial integration, one can show that  $w_{AB}^{\alpha} = -v_{BA}^{\alpha}$ . Then,

$$(w_{AB}^{\alpha} - v_{BA}^{\alpha})(v_{BA}^{\beta})^* = -2v_{BA}^{\alpha}(v_{BA}^{\beta})^* = -\frac{2}{3}v_{BA}^{\alpha}(v_{BA}^{\alpha})^* \delta_{\alpha\beta}, \quad (51)$$

the last step is correct only for a cubic or isotropic body. For such a body, the product of two matrix elements is a real number. From the requirement that  $\text{Re } \sigma_{\alpha\beta}$  and  $\text{Im } \sigma_{\alpha\beta}$  are real numbers, we only require

$$\begin{aligned} & \text{Re}[I_{BA+} \pm I_{BA-}] \\ &= \frac{\sqrt{\pi}\hbar}{2(k_B T \lambda_{BA})^{1/2}} [e^{-\frac{\lambda_{BA}}{4k_B T} [1 + \frac{(\hbar\omega_{BA} - \hbar\omega)}{\lambda_{BA}}]^2} \pm e^{-\frac{\lambda_{BA}}{4k_B T} [1 + \frac{(\hbar\omega_{BA} + \hbar\omega)}{\lambda_{BA}}]^2}] \end{aligned} \quad (52)$$

in expression (1). The temperature dependence (52) is the same as that obtained from the kinetic method,<sup>6</sup> although the Landau-Peierls condition is *not* satisfied. This is a coincidence caused by two factors. First, for LE, EL, LL, and EE transitions driven by external field, the contribution to conductivity has the form of Eq. (1). Thus, only the real part of the one-dimensional time integral plays a role. In contrast to Eq. (4), in the corresponding kinetic expression,<sup>6</sup> the upper limit of time integral is  $\infty$  (long-time limit) rather than 0. Second, because in both cases we apply an asymptotic expansion to calculate the time integral at high temperature, at leading order, the real part of (4) is half the corresponding time integral in kinetic theory. The difference in temperature dependence only appears in subdominant terms.

When transfer integrals or e-ph interaction are involved at first order, various transport processes are the same order

of magnitude as the processes discussed here (zero order in residual interaction). In these first-order processes, it is the imaginary part of a twofold time integral that contribute to conductivity (cf. Ref. 7). Some of these first-order processes do not appear in kinetic models. Even for the processes expected from kinetic theory, the temperature dependence derived in the MRM is different from that derived from kinetic theory.

#### 5. Summation over electronic states

To carry out the sum over the final extended states and average over initial localized states, we first carry out  $\sum_B$  for a fixed localized state  $A$ . We take the center  $\mathbf{R}_A$  of  $\phi_A(\mathbf{r} - \mathbf{R}_A)$  as the origin of coordinates, the incident direction  $\mathbf{k}/|\mathbf{k}|$  of electromagnetic wave as polar axis ( $z$  axis), the directions  $(\epsilon_1, \epsilon_2)$  of two linear polarization vectors as  $x$  and  $y$  axis, respectively. The incident field is expressed as

$$\mathbf{F} = F_1 \epsilon_1 + F_2 \epsilon_2 + 0\mathbf{k}/|\mathbf{k}|. \quad (53)$$

Consider an extended state (a wave packet propagating along  $\mathbf{p}$ )  $V^{-1/2} e^{i\mathbf{p}\cdot\mathbf{r}/\hbar}$ , here for simplicity we neglected other waves with wave vectors close to  $\mathbf{p}$ . We can select an orthogonal frame  $(\mathbf{l}, \mathbf{m}, \mathbf{n})$ , where  $\mathbf{n} = \mathbf{p}/|\mathbf{p}|$ ,  $\mathbf{l}$ , and  $\mathbf{m}$  are two unit vectors perpendicular to each other and perpendicular to  $\mathbf{n}$ . The position vector  $\mathbf{r}$  of electron can be resolved as

$$\mathbf{r} = r_{\perp 1} \mathbf{l} + r_{\perp 2} \mathbf{m} + r_{\parallel} \mathbf{n}. \quad (54)$$

According to Eq. (50), one has

$$\langle \chi_B | \mathbf{r} | \phi_A \rangle = \mathbf{n} \langle \chi_B | r_{\parallel} | \phi_A \rangle. \quad (55)$$

The matrix elements of the perturbation of the external field are simplified to

$$\begin{aligned} \langle \chi_B | \mathbf{F} \cdot \mathbf{r} | \phi_A \rangle &= \mathbf{F} \cdot \mathbf{n} \langle \chi_B | r_{\parallel} | \phi_A \rangle \\ &= \sin\theta (F_1 \cos\phi + F_2 \sin\phi) \frac{i\hbar v_{\parallel}^{BA}}{(E_A - E_B)}, \end{aligned} \quad (56)$$

where  $\theta$  is the inclination angle of  $\mathbf{p}$  relative to  $\mathbf{k}$ , and  $\phi$  is the azimuth angle of the orthogonal projection of  $\mathbf{p}$  on plane  $(\epsilon_1, \epsilon_2)$  relative to  $\epsilon_1$ . In this coordinate system,

$$\sum_{B_1} \rightarrow \frac{V}{(2\pi\hbar)^3} \int_0^{\infty} dp p^2 \int_0^{\pi} d\theta \sin\theta \int_0^{2\pi} d\phi. \quad (57)$$

The incident field (53) has only  $x$  and  $y$  components. So that only the  $xx$ ,  $xy$ ,  $yx$ , and  $yy$  components of the conductivity tensor are involved in the conduction process driven by field (53). In consonance with Eq. (56), one should make the substitution

$$v_{BA}^x \rightarrow v_{\parallel}^{BA} \sin\theta \cos\phi, \quad v_{BA}^y \rightarrow v_{\parallel}^{BA} \sin\theta \sin\phi \quad (58)$$

in the conductivity tensor (1). The angular part of integral (57) can be carried out. From Eqs. (57) and (58), one can see  $\sigma_{xy} = \sigma_{yx} = 0$  and  $\sigma_{xx} = \sigma_{yy} = \sigma$ . Because the factors in Eq. (1) do not depend on the position of localized state  $\phi_A$ , one can carry out the spatial integral in  $\sum_A$ . The conductivity



from LE transitions is

$$\begin{aligned} \begin{cases} \text{Re} \\ \text{Im} \end{cases} \sigma(\omega) &= \frac{4\pi\bar{\xi}^3}{3} \frac{bZe^2 n_{\text{loc}}}{4\pi\epsilon_0\epsilon U} \frac{8ne^2}{3\pi\hbar^3 m^2} \int_0^\infty d\xi \int_0^\infty dp [1 - f(E_{B_1})] f(E_A) \frac{p^4}{(E_{B_1}^0 - E_A^0)} \frac{\xi \exp(-\frac{bZe^2}{4\pi\epsilon_0\epsilon U\xi})}{(1 + p^2\xi^2/\hbar^2)^4} \\ &\times \frac{\sqrt{\pi\hbar}}{2(k_B T \lambda_{BA})^{1/2}} [e^{-\frac{\lambda_{BA}}{4k_B T} (1 + \frac{\hbar\omega_{BA} - \hbar\omega}{\lambda_{BA}})^2} \pm e^{-\frac{\lambda_{BA}}{4k_B T} (1 + \frac{\hbar\omega_{BA} + \hbar\omega}{\lambda_{BA}})^2}], \end{aligned} \quad (59)$$

where  $n = N_e/\Omega_s$  is the carrier concentration, and  $E_A$  and  $E_{B_1}$  are given in Eqs. (15) and (20). From Eq. (59), one can easily compute TCR:  $\rho^{-1} \frac{d\rho}{dT} = -\sigma^{-1} \frac{d\sigma}{dT}$ , an important material parameter for bolometer.<sup>1,55</sup>  $\sigma$  and TCR are expressed with easy access quantities:  $U$  and  $E_c$  for localized states,  $\epsilon$  and  $q_{\text{TF}}$  for the interaction between electron and atomic core, and the averaged sound speed  $\bar{c}$  for the vibrations.

### B. EL transitions driven by external field

Since the field-matter coupling is Hermitian, the corresponding expressions for EL transition driven by field can be obtained from those for LE transitions driven by field through exchanging the status of  $\phi_A$  and  $\chi_B$ :

$$\begin{aligned} \begin{cases} \text{Re} \\ \text{Im} \end{cases} \sigma(\omega) &= \frac{4\pi\bar{\xi}^3}{3} \frac{bZe^2 n_{\text{loc}}}{4\pi\epsilon_0\epsilon U} \frac{8ne^2}{3\pi\hbar^3 m^2} \int_0^\infty d\xi \int_0^\infty dp [1 - f(E_A)] f(E_B) \frac{p^4}{(E_A^0 - E_B^0)} \frac{\xi \exp(-\frac{bZe^2}{4\pi\epsilon_0\epsilon U\xi})}{(1 + p^2\xi^2/\hbar^2)^4} \\ &\times \frac{\sqrt{\pi\hbar}}{2(k_B T \lambda_{AB})^{1/2}} [e^{-\frac{\lambda_{AB}}{4k_B T} (1 + \frac{\hbar\omega_{AB} - \hbar\omega}{\lambda_{AB}})^2} \pm e^{-\frac{\lambda_{AB}}{4k_B T} (1 + \frac{\hbar\omega_{AB} + \hbar\omega}{\lambda_{AB}})^2}], \end{aligned} \quad (60)$$

where

$$y_{\pm}^{AB} = \frac{(\omega_{BA} \pm \omega)^2}{4\lambda_{AB} k_B T}, \quad \lambda_{AB} = \frac{1}{2} \sum_{\alpha} \hbar\omega_{\alpha} (\theta_{\alpha}^A)^2. \quad (61)$$

For the LE transition driven by the transfer integral and the EL transition driven by e-ph interaction, one does not have this symmetry.<sup>6,7</sup>

### C. LL transition driven by external field

One can similarly find the conductivity from the LL transitions driven by external field [Fig. 2(a) of Ref. 7]:

$$\begin{cases} \text{Re} \\ \text{Im} \end{cases} \sigma_{\alpha\beta}(\omega) = -\frac{N_e e^2}{2\Omega_s} \sum_{AA_1} \text{Im} \frac{(w_{AA_1}^{\alpha} - v_{A_1 A}^{\alpha})(v_{A_1 A}^{\beta})^*}{(E_A^0 - E_{A_1}^0)} i[I_{A_1 A+} \pm I_{A_1 A-}] [1 - f(E_{A_1})] f(E_A), \quad (62)$$

where the velocity matrix elements are

$$w_{AA_1}^{\alpha} = -\frac{i\hbar}{m} \int d^3x \phi(\mathbf{r} - \mathbf{R}_A) \frac{\partial}{\partial x_{\alpha}} \phi^*(\mathbf{r} - \mathbf{R}_{A_1}) \quad (63)$$

and

$$v_{A_1 A}^{\alpha} = -\frac{i\hbar}{m} \int d^3x \phi^*(\mathbf{r} - \mathbf{R}_{A_1}) \frac{\partial}{\partial x_{\alpha}} \phi(\mathbf{r} - \mathbf{R}_A). \quad (64)$$

$v_{A_1 A}^{\alpha}$  is given in Eq. (A2) and  $w_{AA_1}^{\alpha} = -v_{A_1 A}^{\alpha}$ . The time integral

$$\begin{aligned} I_{A_1 A\pm}(\omega) &= \exp \left\{ -\frac{1}{2} \sum_{\alpha} (\theta_{\alpha}^{A_1} - \theta_{\alpha}^A)^2 \coth \frac{\beta\hbar\omega_{\alpha}}{2} \right\} \int_{-\infty}^0 ds e^{\pm i\omega s} e^{-is(E_{A_1}' - E_A')/\hbar} \\ &\times \exp \left[ \frac{1}{2} \sum_{\alpha} \frac{(\theta_{\alpha}^{A_1} - \theta_{\alpha}^A)^2}{2} \left( \coth \frac{\beta\hbar\omega_{\alpha}}{2} \cos \omega_{\alpha} s + i \sin \omega_{\alpha} s \right) \right] \end{aligned} \quad (65)$$

contains the primary temperature dependence of conductivity. At high temperature  $k_B T \geq \hbar\bar{\omega}$ ,  $I_{A_1 A\pm}$  reduces to

$$I_{A_1 A\pm}(\omega) = -i\hbar/\lambda_{A_1 A} + \frac{\hbar e^{-\beta\hbar(\pm\omega + \omega_{AA_1})/2 - y_{\pm}^{A_1 A} - \beta\lambda_{A_1 A}/4}}{(\lambda_{A_1 A} k_B T)^{1/2}} \left[ \frac{\sqrt{\pi}}{2} - iA(y_{\pm}^{A_1 A}) \right], \quad (66)$$

where

$$\lambda_{A_1 A} = \frac{1}{2} \sum_{\alpha} \hbar\omega_{\alpha} (\theta_{\alpha}^{A_1} - \theta_{\alpha}^A)^2 \quad (67)$$

and

$$y_{\pm}^{A_1 A} = \frac{[\hbar(\pm\omega + \omega_{AA_1})]^2}{4\lambda_{A_1 A} k_B T}. \quad (68)$$

To carry out the summation over initial and final electronic states, we first fix the initial electronic state  $A$ . We take the center  $\mathbf{R}_A$  of localized state  $\phi_A(\mathbf{r} - \mathbf{R}_A)$  as the origin and the incident direction  $\mathbf{k}$  of the electromagnetic wave as the polar axis. Denote  $R = R_{AA_1} = |\mathbf{R}_{A_1} - \mathbf{R}_A|$  the distance between the centers of localized states  $\phi_{A_1}(\mathbf{r} - \mathbf{R}_{A_1})$  and  $\phi_A$ , and the unit vector along  $(\mathbf{R}_{A_1} - \mathbf{R}_A)$  is  $\mathbf{n}_{AA_1} = (X_{AA_1}, Y_{AA_1}, Z_{AA_1})/R_{AA_1}$ , where  $(X_{AA_1}, Y_{AA_1}, Z_{AA_1})$  are the Cartesian components of vector  $\mathbf{R}_{A_1} - \mathbf{R}_A$ .

Since the conductivity tensor is usually expressed in a system of Cartesian coordinates, we introduce an auxiliary

Cartesian system  $(\epsilon_1, \epsilon_2, \mathbf{k})$ , where  $\epsilon_1$  and  $\epsilon_2$  are the two linear polarization vectors. The electric field  $\mathbf{F}$  has only  $x$  and  $y$  components:  $\mathbf{F} = F_1\epsilon_1 + F_2\epsilon_2 + 0\mathbf{k}$ . Because we sum over  $A_1$ , the centers  $\mathbf{R}_{A_1}$  of localized states  $\phi_{A_1}(\mathbf{r} - \mathbf{R}_{A_1})$  sit at different points. To simplify the calculation of the velocity matrix elements, we resolve the position vector  $\mathbf{r}$  of electron in an orthogonal frame:

$$\mathbf{r} = r_{\perp 1}\mathbf{l}_{AA_1} + r_{\perp 2}\mathbf{m}_{AA_1} + r_{\parallel}\mathbf{n}_{AA_1}, \quad (69)$$

where  $\mathbf{l}_{AA_1}$  and  $\mathbf{m}_{AA_1}$  are two unit vectors perpendicular to each other and to  $\mathbf{n}_{AA_1}$ . From Eq. (A4), one has

$$\langle \phi_{A_1} | \mathbf{r} | \phi_A \rangle = \mathbf{n}_{AA_1} \langle \phi_{A_1} | r_{\parallel} | \phi_A \rangle. \quad (70)$$

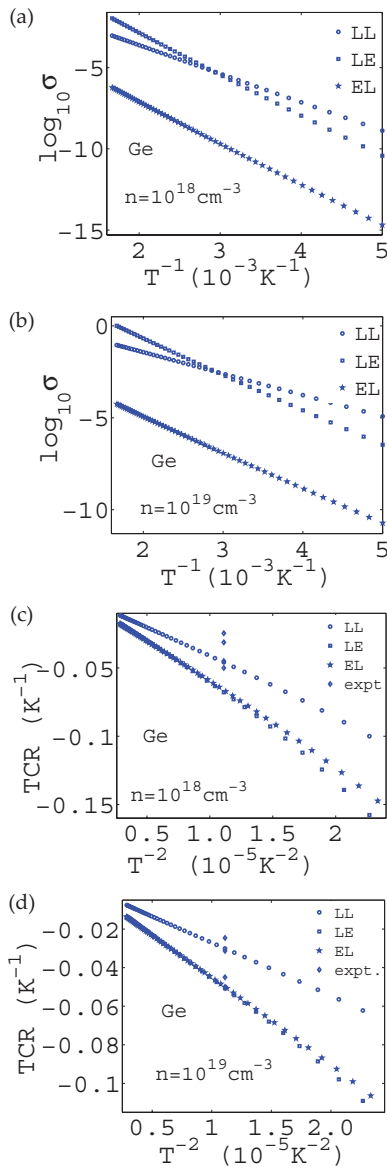


FIG. 4. (Color online) Conductivity and TCR as functions of temperature in two  $n$ -doped  $a$ -Ge:H samples at  $\omega = 0$ . The experimental values are taken from Refs. 47 and 48.

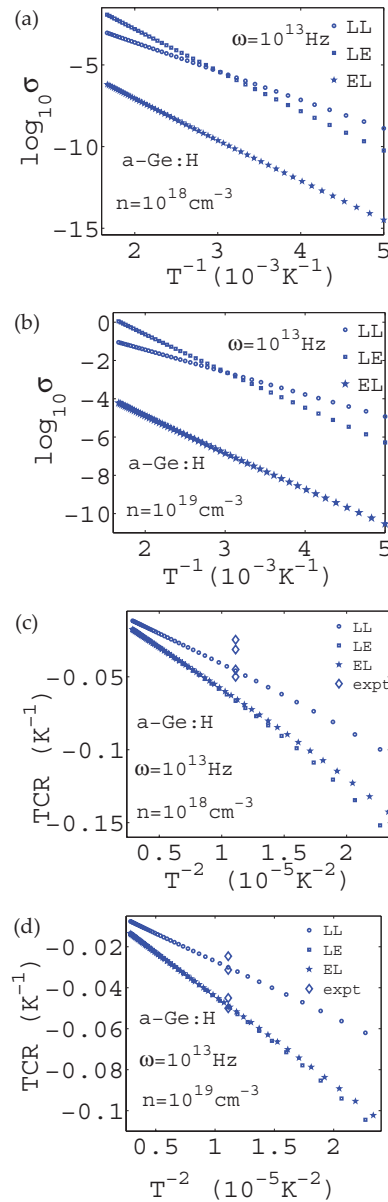


FIG. 5. (Color online) Conductivity and TCR as functions of temperature in two  $n$ -doped  $a$ -Ge:H samples at  $\omega = 10^{13}$  Hz. The experimental values are taken from Refs. 47 and 48.

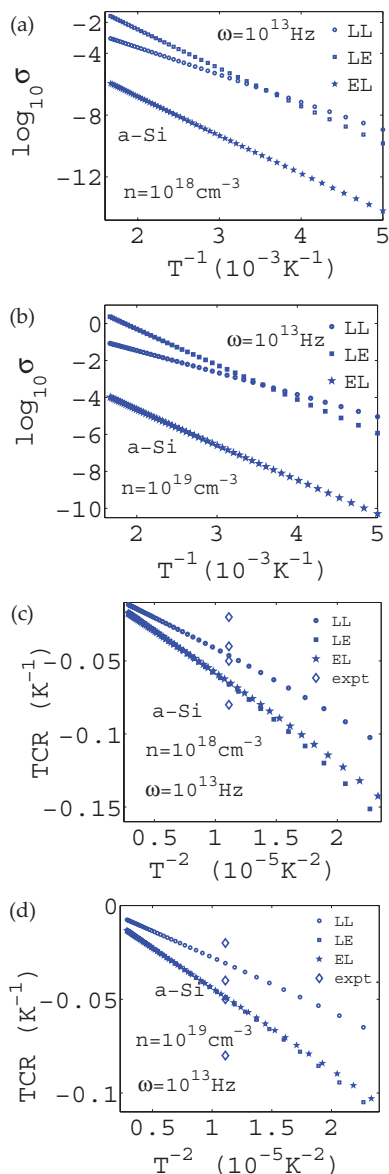


FIG. 6. (Color online) Conductivity and TCR as functions of temperature in two  $n$ -doped  $a$ -Si:H samples at  $\omega = 10^{13}$  Hz. The experimental values are taken from Ref. 55.

By means of Eq. (70), the perturbation of the electric field is

$$\begin{aligned} \langle \phi_{A_1} | \mathbf{F} \cdot \mathbf{r} | \phi_A \rangle &= \mathbf{F} \cdot \mathbf{n}_{AA_1} \langle \phi_{A_1} | r_{\parallel} | \phi_A \rangle \\ &= \sin \theta (F_1 \cos \phi + F_2 \sin \phi) \frac{i \hbar v_{\parallel}^{A_1 A}}{(E_A - E_{A_1})}, \end{aligned} \quad (71)$$

where  $v_{\parallel}^{A_1 A}$  has been obtained in the Appendix. The angular integrals in summation  $\sum_{A_1}$  can be effected:  $\sigma_{xy} = \sigma_{yx} = 0$  and  $\sigma_{xx} = \sigma_{yy} = \sigma$ . Because of the uniformity of AS, the spatial integral in  $\sum_A$  can be carried out. The conductivity

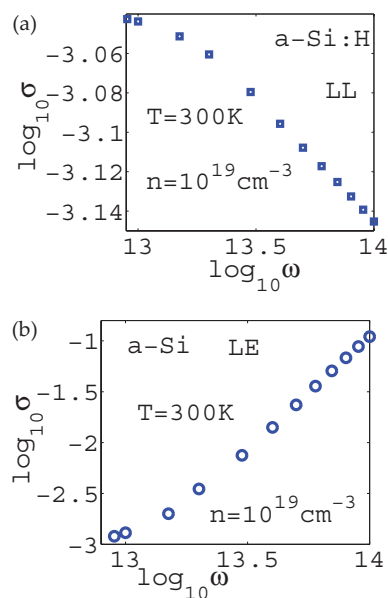


FIG. 7. (Color online) Conductivity as a function of frequency at  $T = 300$  K. (a) LL transition; (b) LE transition. In the frequency range, the contribution from LE transition is more important than that from LL transitions.

from LL transition driven by field is

$$\begin{aligned} &\begin{cases} \text{Re} \\ \text{Im} \end{cases} \sigma(\omega) \\ &= \frac{4\pi \bar{\xi}^3}{3} \left[ \frac{bZe^2 n_{\text{loc}}}{4\pi \epsilon_0 \epsilon U} \right]^2 \int_0^{\infty} \frac{d\xi_1}{\xi_1^2} \exp\left(-\frac{bZe^2}{4\pi \epsilon_0 \epsilon U \xi_1}\right) \\ &\quad \times \int_0^{\infty} \frac{d\xi_2}{\xi_2^2} \exp\left(-\frac{bZe^2}{4\pi \epsilon_0 \epsilon U \xi_2}\right) n e^2 \frac{[1 - f(E_{A_1})] f(E_A)}{2(E_A^0 - E_{A_1}^0)} \\ &\quad \times \frac{\sqrt{\pi} \hbar}{2(\lambda_{A_1 A} k_B T)^{1/2}} \left[ e^{-\frac{\lambda_{A_1 A}}{4k_B T} (1 + \frac{\hbar \omega_{A_1 A} - \hbar \omega}{\lambda_{A_1 A}})^2} \pm e^{-\frac{\lambda_{A_1 A}}{4k_B T} (1 + \frac{\hbar \omega_{A_1 A} + \hbar \omega}{\lambda_{A_1 A}})^2} \right] \\ &\quad \times \int_0^{R_c} R^2 dR \frac{4\pi}{3} (w_{\parallel}^{AA_1} - v_{\parallel}^{A_1 A})(v_{\parallel}^{A_1 A})^*, \end{aligned} \quad (72)$$

where, and in the Appendix, to shorten the symbols, we use  $\xi_2$  instead of  $\xi_{A_1}$  and use  $\xi_1$  instead of  $\xi_A$ .

We can see from Eqs. (59), (60), and (72) that when  $\omega = 0$ ,  $\text{Im} \sigma = 0$  for LL, LE, and EL transitions. For two  $n$ -doped  $a$ -Ge:H samples with  $n = 10^{18}$  and  $10^{19}$   $\text{cm}^{-3}$ ,  $\log_{10} \sigma$  and TCR from LL, LE, and EL transitions as functions of temperature at  $\omega = 0$  are plotted in Fig. 4. The corresponding results at  $\omega = 10^{13}$  Hz are plotted in Fig. 5.  $\text{Re} \sigma$  increases with frequency, while TCR decreases with frequency. For two  $n$ -doped  $a$ -Si:H samples, the conductivity and TCR as functions of temperature at  $\omega = 10^{13}$  Hz are plotted in Fig. 6 (the results at  $\omega = 0$  were reported in Ref. 54). The calculated TCR for  $a$ -Si:H falls<sup>54</sup> in the observed<sup>55,57,58</sup> range between  $-2\%$  and  $-8\%$ .

At  $\omega = 0$ , the conductivity from LE transition is the same order of magnitude as that from LL transitions, and the conductivity from EL transitions is much smaller than those from LL and LE transitions. There is a crossover temperature  $T^*$ , below  $T^*$  the conductivity from LL transitions is larger

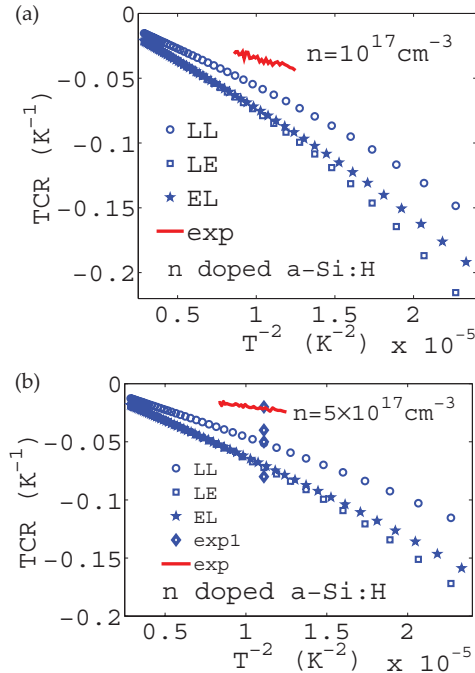


FIG. 8. (Color online) TCR as a function of temperature in two  $n$ -doped  $a$ -Si:H with  $n = 10^{17} \text{ cm}^{-3}$  and  $5 \times 10^{17} \text{ cm}^{-3}$ , the diamond symbol data are taken from Refs. 47 and 48, and the solid line experimental data taken from Ref. 56.

than the conductivity from LE transitions, and above  $T^*$  the conductivity from LE transitions is larger. Because the activation energy for LL transitions is different to that for

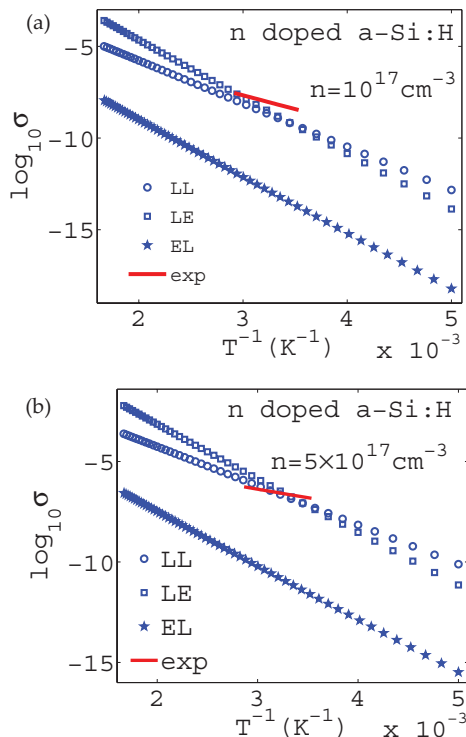


FIG. 9. (Color online) dc conductivity as function of temperature in two  $n$ -doped  $a$ -Si:H with  $n = 10^{17} \text{ cm}^{-3}$  and  $5 \times 10^{17} \text{ cm}^{-3}$ ; experimental data are taken from Ref. 56.

LE transitions, this phenomenon explained the kink on the observed  $\log_{10} \sigma$  versus  $1/T$  curve.<sup>54</sup>

For two  $n$ -doped  $a$ -Si:H samples at 300 K,  $\log_{10} \sigma(\omega)$  versus  $\log_{10} \omega$  in a frequency range  $10^{13}$  to  $10^{14}$  Hz is illustrated in Fig. 7(b). We can see that (i) the conductivity of LL transitions slowly decreases with  $\omega$ ; (ii) the conductivity from LE transitions increases rapidly with frequency. The total conductivity is a sum from various processes,<sup>7</sup> and the conductivity from LL transitions is smaller than that from the LE transitions at higher frequency. The total conductivity arises mainly from LE transitions at higher frequencies. The general trend in  $\log_{10} \sigma(\omega)$  versus  $\log_{10} \omega$  is not far from the Tanaka and Fan<sup>59</sup> result  $\sigma(\omega) \sim \omega^2$ , but obviously deviates from the simple power law around  $10^{13}$  Hz. We must be cautious that the results derived in this work are only suitable to the contributions from electrons: at such high frequency, the ionic contribution should also be included.

In Fig. 8, we compared the observed and calculated TCR for two  $n$ -doped  $a$ -Si:H with  $n = 10^{17} \text{ cm}^{-3}$  and  $5 \times 10^{17} \text{ cm}^{-3}$ . The calculations roughly agree with the experiment<sup>56</sup> in temperature range 282–349 K. The observed absolute values of TCR are systematically smaller than those of the calculated. This is due to the samples containing microcrystalline grains in the amorphous matrix,<sup>55</sup> while crystalline material has smaller absolute value of TCR. Figure 9 shows the comparisons for conductivity.

#### IV. CONCLUSION

The microscopic response method expresses transport coefficients with transition amplitude rather than transition probability per unit time, and may be used in amorphous semiconductors in which the Landau-Peierls condition is violated.<sup>3,4</sup> We presented an approximate theory for the conductivity and Hall mobility in amorphous semiconductors systematically derived from the MRM. We obtained the temperature dependence of the conductivity from the three simplest transitions: LL, LE, and EL transitions driven solely by field [cf. Eqs. (62), (59), and (60)]. The conductivity is expressed in terms of accessible physical quantities: mobility edge, Urbach energy, static dielectric constant, and elastic modulus. LE transition (ignored in previous theories) contributes to conductivity in the same order as LL and EE transitions. Below a crossover temperature  $T^*$ , the conductivity from LL transitions is larger than that from LE transitions; above  $T$ , the conductivity from LE transitions is larger. This phenomenon, and different activation energy for LL and LE transitions, is the reason for the kink in the observed conductivity versus the  $1/T$  curve. We show how a kinetic theory of transport can be properly generalized for AS.

#### ACKNOWLEDGMENTS

We would like to express our deep appreciation to D. B. Saint John and N. J. Podraza for giving us their unpublished resistivity versus temperature data<sup>56</sup> of  $n$ -doped  $a$ -Si:H samples, which made a broader comparison with experiments possible. We thank the US Army Research Laboratory, the US Army Research Office under Grant No. W911NF-11-1-0358, and NSF under Grant No. DMR 09-03225 for support.

### APPENDIX: VELOCITY MATRIX ELEMENTS BETWEEN TWO LOCALIZED STATES

To calculate the velocity matrix elements in Eq. (64), it is convenient to adopt a system of spherical coordinates. We take the center  $\mathbf{R}_A$  of localized state  $\phi_A(\mathbf{r} - \mathbf{R}_A)$  as the origin  $\mathbf{R}_A = 0$ , and the connection line  $\mathbf{R}_{A_1} - \mathbf{R}_A$  between the centers of two localized states as the polar axis. Denote  $r = |\mathbf{r} - \mathbf{R}_A|$  and  $r_2 = |\mathbf{r} - \mathbf{R}_{A_1}| = [r^2 + R^2 - 2rR \cos \theta]^{1/2}$ , where  $R = |\mathbf{R}_{A_1} - \mathbf{R}_A|$  and  $\theta$  is the angle between  $\mathbf{r} - \mathbf{R}_A$  and  $\mathbf{R}_{A_1} - \mathbf{R}_A$ . The  $v_z$  matrix element can be written as

$$v_{A_1 A}^z = -\frac{i\hbar}{m} \pi^{-1} \xi_1^{-3/2} \xi_2^{-3/2} \int_0^\infty r^2 dr \int_0^\pi \sin \theta d\theta \times \int_0^{2\pi} d\phi e^{-r_2/\xi_2} \frac{\partial}{\partial z} e^{-r/\xi_1},$$

$$\begin{aligned} v_{\parallel}^{A_1 A} &= -\frac{i\hbar}{m} \pi^{-1} \xi_1^{-3/2} \xi_2^{-3/2} \int d^3x e^{-r_2/\xi_2} \nabla_{\parallel} e^{-r/\xi_1} = -\frac{i\hbar}{m} (\xi_1 \xi_2)^{-3/2} \left\{ -4 \left( \frac{\xi_2^2}{R^2} + \frac{\xi_2}{R} \right) \frac{e^{-R/\xi_2} \xi_1'^3}{\xi_1} \right. \\ &\quad - \left( 2 + 6 \frac{\xi_2}{R} + 6 \frac{\xi_2^2}{R^2} \right) \frac{\xi_2 e^{-R/\xi_2} \xi_1'^2}{\xi_1} - \left( 2 + 6 \frac{\xi_2}{R} + 6 \frac{\xi_2^2}{R^2} \right) \frac{\xi_2^2 e^{-R/\xi_2} \xi_1'}{\xi_1} \\ &\quad + \left( \frac{2}{\xi_2 R} + \frac{2}{R^2} \right) \frac{\xi_2^2 e^{-R/\xi_2} \xi_1'^3}{\xi_1} [2 - (R^2/\xi_1'^2 + 2R/\xi_1'' + 2)e^{-R/\xi_1''}] \\ &\quad - \left( \frac{2}{\xi_2} + \frac{6}{R} + 6 \frac{\xi_2}{R^2} \right) \frac{\xi_2^2 e^{-R/\xi_2} \xi_1'^2}{\xi_1} [1 - (R/\xi_1'' + 1)e^{-R/\xi_1''}] + \left( 2 + 6 \frac{\xi_2}{R} + 6 \frac{\xi_2^2}{R^2} \right) \frac{\xi_2^2 e^{-R/\xi_2} \xi_1''}{\xi_1} (1 - e^{-R/\xi_1''}) \\ &\quad + \left( \frac{2}{R^2} - \frac{2}{R\xi_2} \right) \frac{\xi_2^2 e^{-R/\xi_1} \xi_1'^3}{\xi_1} \left( \frac{R^2}{\xi_1'^2} + 2 \frac{R}{\xi_1'} + 2 \right) + \left( \frac{6\xi_2}{R^2} + \frac{2}{\xi_2} - \frac{6}{R} \right) \frac{\xi_2^2 e^{-R/\xi_1} \xi_1'^2}{\xi_1} \left( \frac{R}{\xi_1'} + 1 \right) \\ &\quad \left. + \left( 2 - 6 \frac{\xi_2}{R} + 6 \frac{\xi_2^2}{R^2} \right) \frac{\xi_2^2 e^{-R/\xi_1} \xi_1'}{\xi_1} \right\}, \end{aligned} \quad (\text{A2})$$

where  $\xi_1'$  and  $\xi_1''$  are defined by

$$\xi_1'^{-1} = \xi_1^{-1} + \xi_2^{-1} \quad \text{and} \quad \xi_1''^{-1} = \xi_1^{-1} - \xi_2^{-1}.$$

Equation (A2) displays the exponential decay of velocity matrix elements with distance  $R$  between two localized states. In the variable range hopping argument,<sup>2</sup> only the exponential decay of transfer integral with  $R$  is treated. In a process that is first order in transfer integral, which is not discussed here, one may expect interesting new features.

and one has similar expressions for the matrix elements of  $v_x$  and  $v_y$ . Because  $r_2$  does not depend on the azimuth angle  $\phi$ ,

$$v_{A_1 A}^x = v_{A_1 A}^y = 0. \quad (\text{A1})$$

We condense them as  $v_{\perp}^{A_1 A} = 0$ : the matrix element for any component of velocity perpendicular to the connection line between two localized states is zero.

The  $\phi$  integral is immediate, and the remaining  $r$  and  $\theta$  integrals in  $v_{A_1 A}^z$  can be calculated by changing the integration variable  $\theta$  to  $r_2$  for a fixed  $r$ . With the help of  $\cos \theta = \frac{r^2 + R^2 - r_2^2}{2rR}$  and  $\sin \theta d\theta = \frac{r_2 dr_2}{Rr}$ , the integral over  $\theta$  becomes an integral over  $r_2$ . One first carries out the integral over  $r_2$ , then carries out the integral over  $r$ . For the velocity component parallel to the connection line between two localized states, the matrix element is

Because for each Cartesian component,

$$\langle \phi_{A_1} | v_{\alpha} | \phi_A \rangle = \frac{i\hbar \langle \phi_{A_1} | v_{\alpha} | \phi_A \rangle}{(E_A - E_{A_1})}, \quad \alpha = x, y, z \quad (\text{A3})$$

from (A1) and (A2), one has

$$\langle \phi_{A_1} | r_{\perp} | \phi_A \rangle = 0 \quad \text{and} \quad \langle \phi_{A_1} | r_{\parallel} | \phi_A \rangle = \frac{i\hbar v_{\parallel}^{A_1 A}}{(E_A - E_{A_1})}. \quad (\text{A4})$$

<sup>1</sup>R. A. Street, *Hydrogenated Amorphous Silicon* (Cambridge University Press, Cambridge, UK, 1991).

<sup>2</sup>N. F. Mott and E. A. Davis, *Electronic Processes in Non-crystalline Materials* (Clarendon, Oxford, 1971).

<sup>3</sup>R. Peierls, *Surprises in Theoretical Physics* (Princeton University Press, Princeton, NJ, 1979), pp. 121–126.

<sup>4</sup>R. Peierls, *Quantum Theory of Solids* (Clarendon, Oxford, 1955), pp. 139–142.

<sup>5</sup>E. M. Lifshitz and L. P. Pitaevskii, *Physical Kinetics* (Butterworth-Heinemann, Oxford, 1981).

<sup>6</sup>M.-L. Zhang and D. A. Drabold, *Eur. Phys. J. B.* **77**, 7 (2010).

<sup>7</sup>M.-L. Zhang and D. A. Drabold, *Phys. Status Solidi B* **248**, 2015 (2011).

<sup>8</sup>A. Miller and E. Abrahams, *Phys. Rev.* **120**, 745 (1960).

<sup>9</sup>H. Overhof and P. Thomas, *Electronic Transport in Hydrogenated Amorphous Semiconductor* (Springer-Verlag, Berlin, 1989).

- <sup>10</sup>M.-L. Zhang and D. A. Drabold, *Phys. Rev. Lett.* **105**, 186602 (2010).
- <sup>11</sup>M.-L. Zhang and D. A. Drabold, *Phys. Rev. B* **81**, 085210 (2010).
- <sup>12</sup>P. G. Le Comber and J. Mort, *Electronic and Structural Properties of Amorphous Semiconductors* (Academic, London, 1973).
- <sup>13</sup>W. H. Butler, *Phys. Rev. B* **31**, 3260 (1985).
- <sup>14</sup>J. Banhart, *Phys. Rev. Lett.* **82**, 2139 (1999).
- <sup>15</sup>G. D. Mahan, *Many-Particle Physics*, 2nd ed. (Plenum, New York, 1990).
- <sup>16</sup>W. Beyer and H. Mell, in *Amorphous and Liquid Semiconductors*, edited by W. E. Spear (CICL, Edinburgh, 1977), p. 333.
- <sup>17</sup>M. J. Cliffe, M. T. Dove, D. A. Drabold, and A. L. Goodwin, *Phys. Rev. Lett.* **104**, 125501 (2010).
- <sup>18</sup>L. D. Landau and E. M. Lifshitz, *Theory of Elasticity*, 3rd ed. (Butterworth-Heinemann, London, 1986).
- <sup>19</sup>N. W. Ashcroft and N. D. Mermin, *Solid State Physics* (Holt, Rinehart and Winston, New York, 1976).
- <sup>20</sup>W. A. Kamitakahara, C. M. Soukoulis and H. R. Shanks, U. Buchenau, and G. S. Grest, *Phys. Rev. B* **36**, 6539 (1987).
- <sup>21</sup>L. D. Landau and E. M. Lifshitz, *Mechanics*, 3rd ed. (Butterworth-Heinemann, London, 1976).
- <sup>22</sup>N. F. Mott, *Conduction in Non-Crystalline Materials*, 2nd ed. (Clarendon, Oxford, 1993).
- <sup>23</sup>Y. Pan, M. Zhang, and D. A. Drabold, *J. Non. Cryst. Sol.* **354**, 3480 (2008).
- <sup>24</sup>Y. Pan, F. Inam, M. Zhang, and D. A. Drabold, *Phys. Rev. Lett.* **100**, 206403 (2008).
- <sup>25</sup>D. A. Drabold, Y. Li, B. Cai, and M.-L. Zhang, *Phys. Rev. B* **83**, 045201 (2011).
- <sup>26</sup>J. J. Ludlam, S. N. Taraskin, S. R. Elliott, and D. A. Drabold, *J. Phys.: Condens. Matter* **17**, L321 (2005).
- <sup>27</sup>F. Inam, J. P. Lewis, and D. A. Drabold, *Phys. Status Solidi A* **207**, 599 (2010).
- <sup>28</sup>J. H. Davis, *J. Non-Cryst. Solids* **35**, 67 (1980).
- <sup>29</sup>F. Orapunt and S. K. O'Leary, *J. Appl. Phys.* **104**, 073513 (2008).
- <sup>30</sup>J. Dong and D. A. Drabold, *Phys. Rev. Lett.* **80**, 1928 (1998).
- <sup>31</sup>R. B. Wehrspohn, S. C. Deane, I. D. French, I. G. Gale, M. J. Powell, and R. Brüggemann, *Appl. Phys. Lett.* **74**, 3374 (1999).
- <sup>32</sup>Y.-T. Li and D. A. Drabold (unpublished).
- <sup>33</sup>F. Urbach, *Phys. Rev.* **92**, 1324 (1953).
- <sup>34</sup>S. Aljishi, J. D. Cohen, S. Jin, and L. Ley, *Phys. Rev. Lett.* **64**, 2811 (1990).
- <sup>35</sup>Y. Kanemitsu, M. Iiboshi, and T. Kushida, *Appl. Phys. Lett.* **76**, 2200 (2000).
- <sup>36</sup>M. Ivanda, *Phys. Rev. B* **46**, 14893 (1992).
- <sup>37</sup>Q. Gu, E. A. Schiff, J. B. Chevrier, and B. Equer, *Phys. Rev. B* **52**, 5695 (1995).
- <sup>38</sup>M. Stutzmann and J. Stuke, *Solid State Commun.* **47**, 635 (1983).
- <sup>39</sup>I. Yassievich, M. Bresler, and O. Gusev, *J. Non-Cryst. Solids* **226**, 192 (1998).
- <sup>40</sup>J. A. Howard and R. A. Street, *Phys. Rev. B* **44**, 7935 (1991).
- <sup>41</sup>E. Louis and J. A. Verges, *Solid State Commun.* **60**, 157 (1986).
- <sup>42</sup>B. Velicky, *Phys. Rev.* **184**, 614 (1969).
- <sup>43</sup>M. Zhang, Y. Pan, F. Inam, and D. A. Drabold, *Phys. Rev. B* **78**, 195208 (2008).
- <sup>44</sup>T. Holstein, *Ann. Phys. (NY)* **8**, 325 (1959); **8**, 343 (1959).
- <sup>45</sup>D. A. Drabold, P. A. Fedders, S. Klemm, and O. F. Sankey, *Phys. Rev. Lett.* **67**, 2179 (1991).
- <sup>46</sup>R. Atta-Fynn, P. Biswas, and D. A. Drabold, *Phys. Rev. B* **69**, 245204 (2004).
- <sup>47</sup>A. Torres, A. Kosarev, M. L. Garcia Cruz, and R. Ambrosio, *J. Non-Cryst. Solids* **329**, 179 (2003).
- <sup>48</sup>A. Inoue, M. Yamamoto, H. M. Kimura, and T. Masumoto, *J. Mater. Sci. Lett.* **6**, 194 (1987).
- <sup>49</sup>D. A. Greenwood, *Proc. Phys. Soc.* **71**, 585 (1958).
- <sup>50</sup>C. M. Bender and S. A. Orszag, *Advanced Mathematical Methods For Scientists and Engineers* (McGraw-Hill, New York, 1978).
- <sup>51</sup>S. K. Bahl and N. Bluzer, in *Tetrahedrally Bonded Amorphous Semiconductors*, edited by M. H. Brodsky, S. Kirkpatrick, and D. Weaire (AIP, New York, 1974), p. 320.
- <sup>52</sup>M. H. Brodsky and A. Lurio, *Phys. Rev. B* **9**, 1646 (1974).
- <sup>53</sup>M. C. Payne, A. F. J. Levit, W. A. Phillips, J. C. Inkson, and C. J. Adkins, *J. Phys. C: Solid State Phys.* **17**, 1643 (1984).
- <sup>54</sup>M.-L. Zhang and D. A. Drabold, e-print [arXiv:1112.2169v2](https://arxiv.org/abs/1112.2169v2) [cond-mat.stat-mech], *Europhys. Lett.*, in press.
- <sup>55</sup>D. B. Saint John, H.-B. Shin, M.-Y. Lee, S. K. Ajmera, A. J. Syllaios, E. C. Dickey, T. N. Jackson, and N. J. Podraza, *J. Appl. Phys.* **110**, 033714 (2011).
- <sup>56</sup>D. B. Saint John, H.-B. Shin, M.-Y. Lee, S. K. Ajmera, A. J. Syllaios, E. C. Dickey, T. N. Jackson, and N. J. Podraza (unpublished).
- <sup>57</sup>A. Orduna-Diaz, C. G. Trevino-Palacios, M. Rojas-Lopez, R. Delgado-Macuilb, V. L. Gayoub, and A. Torres-Jacomea, *Mater. Sci. Eng. B* **174**, 93 (2010).
- <sup>58</sup>P. W. Kruse, *Uncooled Thermal Imaging: Arrays, Systems, and Applications* (SPIE, Bellingham, WA, 2001).
- <sup>59</sup>S. Tanaka and H. Y. Fan, *Phys. Rev.* **132**, 1516 (1963).